International Journal of Engineering Research and Development
e-ISSN: 2278-067X, p-ISSN: 2278-800X, www.ijerd.com
Volume 8, Issue 12 (October 2013), PP. 06-18

Numerical modelling of heat transfer in a channel with transverse baffles

M.A. Louhibi[1], N. Salhi[1], H. Bouali[1], S. Louhibi[2]
[1]*Laboratoire de Mécanique et Energétique, Faculté des Sciences, BP. 717 Boulevard Mohamed VI - 60000 Oujda, Maroc.*
[2]*Ecole National des sciences Appliquées, Boulevard Mohamed VI - 60000 Oujda, Maroc.*

Abstract:- In this work, forced convection heat transfer inside a channel of rectangular section, containing some rectangular baffle plates, is numerically analyzed. We have developed a numerical model based on a finite-volume method, and we have solved the coupling pressure-velocity by the SIMPLE algorithm [6]. We show the effects of various parameters of the baffles, such as, baffle's height, location and number on the isotherms, streamlines, temperatures distributions and local Nusselt number values. It is concluded that: I) The baffles location and height has a meaningful effect on isotherms, streamlines and total heat transfer through the channel. (II) The heat transfer enhances with increasing both baffle's height and number.

Keywords:- Forced convection, Baffles, Finite volume method, Simple, Quick, k-ε

I. INTRODUCTION

In recent years, a large number of experimental and numerical works were performed on turbulent forced convection in heat exchangers with different type of baffles [1-4]. This interest is due to the various industrial applications of this type of configuration such as cooling of nuclear power plants and aircraft engine ... etc.
S. . V Patankar and EM Sparrow [1] have applied a numerical solution procedure in order to treat the problem of fluid flow and heat transfer in fully developed heat exchangers. These one was equipped by isothermal plate placed transversely to the direction of flow. They found that the flow field is characterized by strong recirculation zones caused by solid plates. They concluded that the Nusselt number depends strongly on the Reynolds number, and it is higher in the case of fully developed then that of laminar flow regime.

Demartini et al [2] conducted numerical and experimental studies of turbulent flow inside a rectangular channel containing two rectangular baffles. The numerical results were in good agreement with those obtained by experiment. They noted that the baffles play an important role in the dynamic exchangers studied. Indeed, regions of high pressure 'recirculation regions' are formed nearly to chicanes.
Recently, Nasiruddin and Siddiqui [3] studied numerically effects of baffles on forced convection flow in a heat exchanger. The effects of size and inclination angle of baffles were detailed. They considered three different arrangements of baffles. They found that increasing the size of the vertical baffle substantially improves the Nusselt number. However, the pressure loss is also important. For the case of inclined baffles, they found that the Nusselt number is maximum for angles of inclination directed downstream of the baffle, with a minimum of pressure loss.
More recently, Saim et al [4] presented a numerical study of the dynamic behavior of turbulent air flow in horizontal channel with transverse baffles. They adapted numerical finite volume method based on the SIMPLE algorithm and chose

□ □ε model for treatment of turbulence. Results obtained for a case of such type, at low Reynolds number, were presented in terms of velocity and temperature fields. They found the existence of relatively strong recirculation zones near the baffles. The eddy zones are responsible of local variations in the Nusselts numbers along the baffles and walls.

We know that the primary heat exchanger goal is to efficiently transfer heat from one fluid to another separated, in most practical cases, by solid wall. To increase heat transfer, several approaches have been proposed. We can cite the specific treatment of solid separation surface (roughness, tube winding, vibration, etc.). This transfer can also be improved by creation of longitudinal vortices in the channel. These eddies are produced by introducing one or more transverse barriers (baffle plates) inside the channel. The formation of these vortices downstream of baffles causes recirculation zones capable of rapid and efficient heat transfer between solid walls and fluid flow. It is this approach that we will follow in this study. Indeed, we are interested in this work on the numerical modeling of dynamic and thermal behavior of turbulent forced convection in horizontal channel where two walls are raised to a high temperature. This channel may contain one or several rectangular baffles.

A special interest is given to the influence of different parameters, such as height, number and baffle positions on heat transfer and fluid flow.

II. MATHEMATICAL FORMULATION

The geometry of the problem is shown schematically in Figure 1. It is a rectangular duct with isothermal horizontal walls, crossed by a stationary turbulent flow. The physical properties are considered to be constants.

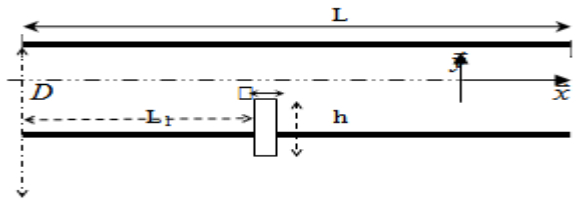

Figure 1: The studied channel

At each point of the flow the velocity has components (u, v) in the x and y directions, and the temperature is denoted T. The turbulence modeling is handled by the classical model (k-ε). k is the turbulent kinetic energy and ε the viscous dissipation of turbulence.

The Transport equations (continuity, momentum, temperature, turbulent kinetic energy and dissipation of turbulence) governing the system, are written in the following general form :

$$\frac{\partial(\rho u\phi)}{\partial x}+\frac{\partial(\rho v\phi)}{\partial y}=\frac{\partial\left[\Gamma_\phi\frac{\partial\phi}{\partial x}\right]}{\partial x}+\frac{\partial\left[\Gamma_\phi\frac{\partial\phi}{\partial y}\right]}{\partial y}+S_\phi \quad (1)$$

Where ρ is the density of the fluid passing through the channel and ϕ, F_φ and S_φ are given by:

Equations	ϕ	Γ_ϕ	S_ϕ
Continuité	1	0	0
Quantité de mouvement selon x	u	$\mu+\mu_t$	$-\frac{\partial P}{\partial x}$

Quantité de mouvement selon y	v	$\mu + \mu_t$	$-\frac{\partial P}{\partial y}$
Energie totale	T	$\mu + \frac{\mu_t}{\sigma_T}$	0
Energie cinétique turbulente	k	$\mu + \frac{\mu_t}{\sigma_k}$	$-\rho.\varepsilon + G$
Dissipation turbulente	ε	$\mu + \frac{\mu_t}{\sigma_\varepsilon}$	$(C_1 G - C_2 \rho\varepsilon)\frac{\varepsilon}{k}$

With : $G = \mu_t \left\{ 2\left[\frac{\partial u}{\partial x}\right]^2 + 2\left[\frac{\partial v}{\partial y}\right]^2 + \left[\frac{\partial v}{\partial x} + \frac{\partial u}{\partial y}\right]^2 \right\}$ μ and μ_t represent, respectively, the dynamic and turbulent viscosities.

$$\mu_t = \rho.C_\mu \frac{k^2}{\varepsilon}$$

The constants used in the turbulence model (k-Ɛ) Are those adopted by Chieng and Launder (1980) [8] :

C_μ	C_1	C_2	σ_T	σ_k	σ_ε
0,09	1,44	1,92	0,9	1	1,3

Boundary conditions :

At the channel inlet:

$u = U_{in}$; $v = 0$ and $T = T_{in}$

$k = 0{,}005\, U_{in}^2$ *and* $\varepsilon = 0{,}1 k^{3/2}$

At solid walls:

$u = v = 0$; $k = \varepsilon = 0$ *and* $T = T_w \succ T_{in}$

At the channel exits:

The gradient of any quantity, with respect to the longitudinal direction x is nul.

Our goal is to determine velocity and temperature fields, as well as the turbulence parameters. Particular attention is given to the quantification parameters reflecting heat exchanges such as the Nusselt number (local and average).

III. NUMERICAL FORMULATION

The computer code that we have developed is based on the finite volume method. Computational domain is divided into a number of stitches. To choose the number of cells used in this study, we performed several simulations on a channel (with or without baffles). Finally, we have opted for a 210 × 90 meshes.

The mesh dimensions are variables; they tighten at the solid walls neighborhoods. Consequently, the stitch density is higher near the hot walls and baffles.

We consider a mesh having dimensions Δx and Δy. In the middle of each volume we consider the points P, called centers of control volumes. E, W, N, S are

the centers of the adjacent control volumes. We also consider centers, EE; WW, NN, SS. The faces of each control volume are denoted e, w, n, s.

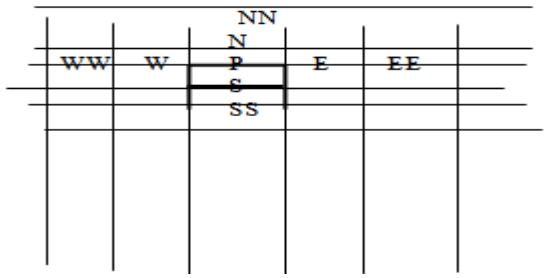

Figure 2: Mesh with P at center

By integrating the transport equation (1) of ϕ on the control volume, we find, a relation to the x direction:

$$[\rho u \phi]_e - [\rho u \phi]_w = \left[\Gamma \frac{d\phi}{dx}\right]_e - \left[\Gamma \frac{d\phi}{dx}\right]_w + [S_\phi]_P$$

Où $[S_\phi]_P$ is the source term.

One note $F = \rho u$, the convection flow and $D = \Gamma / \Delta x$, the diffusion coefficient. And with taking :

$F_e = [\rho u]_e$; $F_w = [\rho u]_w$

$D_e = [\Gamma / \Delta x]_e$; $D_w = [\Gamma / \Delta x]_w$

And : $[d\phi]_e = \phi_E - \phi_P$; $[d\phi]_w = \phi_P - \phi_W$

We found :

$$F_e \phi_e - F_w \phi_w = D_e(\phi_E - \phi_P) - D_w(\phi_P - \phi_W) + [S_\phi]_P$$

To estimate ϕ on the faces " e " and " w " we opted for the classical quick scheme [5] which is a quadratic forms using three nodes. The choice of these nodes is dictated by the direction of flow on these faces $(u \succ 0 \; or \; u \prec 0)$.

Finally, the transport equation (1) is discretized on the mesh with P at center as :

$$a_P \phi_P = a_W \phi_W + a_E \phi_E + a_{WW} \phi_{WW} + a_{EE} \phi_{EE} + [S_\phi]_P \qquad (2)$$

With :

$$\begin{cases} a_W = D_w + \frac{6}{8}\alpha_w F_w + \frac{1}{8}\alpha_e F_e + \frac{3}{8}(1-\alpha_w)F_w \\ a_{WW} = -\frac{1}{8}\alpha_w F_w \\ a_E = D_e - \frac{3}{8}\alpha_e F_e - \frac{6}{8}(1-\alpha_e)F_e - \frac{1}{8}(1-\alpha_w)F_w \\ a_{EE} = \frac{1}{8}(1-\alpha_e)F_e \\ a_P = a_W + a_{WW} + a_E + a_{EE} - [S_\phi]_P \end{cases}$$

Where : $\alpha_e = 1 \, ou \, 0$, $si \quad F_e \succ 0 \, ou \, F_e \prec 0$

$\alpha_w = 1 \, ou \, 0$, $si \quad F_w \succ 0 \, ou \, F_w \prec 0$

The same thing is done for the vertical "y" direction, using the faces "n" and "s" and by introducing the Quick diagram nodes N, NN, S and SS.
if convection flow and diffusion coefficient of the sides "e", "w", "s", "n" are known And especially the source term $\left[S_\phi\right]_p$, the solution of equation (2) then gives us the values of ϕ in different P nodes.
One notes that to accelerate the convergence of equation (2) we have introduced a relaxation factor :

$$\frac{a_P}{\beta}\phi_P = a_W\,\phi_W + a_E\,\phi_E + a_{WW}\,\phi_{WW} + a_{EE}\,\phi_{EE} + \left[S_\phi\right]_P + \frac{1-\beta}{\beta}a_P\phi_P^0 \qquad (3)$$

Where ϕ_P^0 is the value of ϕ_P in the previous step.

The source term appears especially in the conservation of momentum equations in the form of a pressure gradient which is in principle unknown. To get around this coupling we have chosen to use in our code the "Simple" algorithm developed by Pantankar [7]. The basic idea of this algorithm is to assume a field of initial pressure and inject it into the equations of conservation of momentum. Then we solve the system to find a field of intermediate speed (which is not fair because the pressure isn t.) The continuity equation is transformed into a pressure correction equation. This last is determined to find a pressure correction that will inject a new pressure in the equations of motion. The cycle is repeated as many times as necessary until a pressure correction equal "zero" corresponding to the algorithm convergence. In the end we solve the transport equations of T, k and Ɛ.

In this approach, a problem is encountered. It is known as the checkerboard problem.

The risk is that a pressure field can be highly disturbed by the sensed formulation which comprises performing a linear interpolation for estimate the pressure value on the facets of the control volume. To circumvent this problem we use the so-called staggered grids proposed by Harlow and Welch [6]. In this technique, a first grid pressure (and other scalar quantities T, k and Ɛ) is placed in the center of the control volume. While other staggered grids are adopted for the velocity components u and v (see Figure 3).

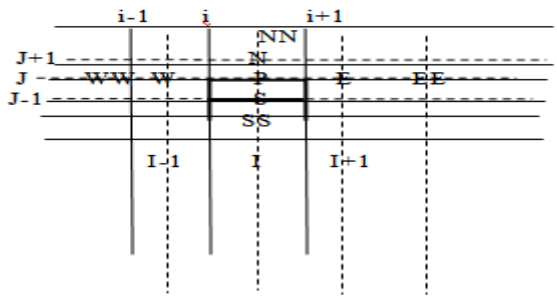

Figure 3: Shifted mesh

The scalar variables, including pressure, are stored at the nodes (I, J). Each node (I, J) is surrounded by nodes E, W, S and N. The horizontal velocity component u is stored on faces "e" and "w", while the vertical component v is stored on the faces denoted "n" and "s".

So the control volume for pressure and other scalar quantities T, k and Ɛ is $\left[(i+1,\,j);(i+1,\,j+1);(i,\,j+1);(i,\,j)\right]$

For component u control volume is
$\left[(I, j);(I, j+1);(I-1, j+1);(I-1, j)\right]$.

While for the v component we use: $\left[(i+1, J-1);(i+1, J);(i, J);(i-1, J-1)\right]$.

By integrating the conservation momentum equation in the horizontal direction on the volume $\left[(I, j);(I, j+1);(I-1, j+1);(I-1, j)\right]$, we found :

$$a_{i,J}u_{i,J} = \sum a_{nb}u_{nb} + \left[P(I-1,J) - P(I,J)\right](y_{j+1} - y_j) \quad (4)$$

Where : $\sum a_{nb}u_{nb} = a_{WW}u_{WW} + a_W u_W + a_{EE}u_{EE} + a_E u_E + a_{SS}u_{SS} + a_S u_S + a_{NN}u_{NN} + a_N u_N$ The coefficients a_{nb} are determined by the quick scheme mentioned above.

Similarly, the integration of conservation momentum equation in the vertical direction on the volume
$\left[(i+1, J-1);(i+1, J);(i, J);(i-1, J-1)\right]$, gives us :

$$a_{I,j}v_{I,j} = \sum a_{nb}v_{nb} + \left[P(I,J-1) - P(I,J)\right](x_{i+1} - x_i) \quad (5)$$

One considers primarily an initial pressure field P^*. The provisional solution of the equations (4) and (5) will be denoted u^* and v^*. We note that u^* and v^* doesn't checks the continuity equation, and:

$$a_{i,J}u^*_{i,J} = \sum a_{nb}u^*_{nb} + \left[P^*(I-1,J) - P^*(I,J)\right](y_{j+1} - y_j) \quad (6-a)$$

$$a_{I,j}v^*_{I,j} = \sum a_{nb}v^*_{nb} + \left[P^*(I,J-1) - P^*(I,J)\right](x_{i+1} - x_i) \quad (6-b)$$

At this stage any one of the three variables is correct. They require correction :

$$\begin{cases} p' = P - P^* \\ u' = u - u^* \\ v' = v - v^* \end{cases} \quad (7)$$

Injecting (7) in equations (4), (5) and (6) we find :

$$a_{i,J}u'_{i,J} = \sum a_{nb}u'_{nb} + \left[P'(I-1,J) - P'(I,J)\right](y_{j+1} - y_j) \quad (8-a)$$

$$a_{I,j}v'_{I,j} = \sum a_{nb}v'_{nb} + \left[P'(I,J-1) - P'(I,J)\right](x_{i+1} - x_i) \quad (8-b)$$

At this level, an approximation is introduced. In order to linearize the equations (8), the terms $\sum a_{nb} u'_{nb}$ and $\sum a_{nb} v'_{nb}$ are simply neglected.

Normally these terms must cancel at the procedure convergence. That is to say that this omission does not affect the final result. However, the convergence rate is changed by this simplification. It turns out that the correction P' is overestimated by the Simple algorithm and the calculation tends to diverge. The remedy to stabilize the calculations is to use a relaxation factor.

We Note that a further treatment of these terms is proposed in the so-called algorithms "SIMPLER" and "SIMPLEC" [7].

The equations (8) become:

$$u'_{i,J} = d_{iJ}\left[P'(I-1,J) - P'(I,J)\right] \quad (9-a)$$

$$v'_{I,j} = d_{Ij}\left[P'(I,J-1) - P'(I,J)\right] \quad (9-b)$$

Avec : $d_{iJ} = \dfrac{y_{j+1} - y_j}{a_{iJ}}$ et $d_{Ij} = \dfrac{x_{i+1} - x_i}{a_{Ij}}$

With :

$$d_{iJ} = \frac{y_{j+1} - y_j}{a_{iJ}} \text{ and } d_{Ij} = \frac{x_{i+1} - x_i}{a_{Ij}}$$

Equations (9) give the corrections to apply on velocities through the formulas (7). We have therefore :

$$u_{i,J} = u^*_{i,J} + d_{iJ}\left[P'(I-1,J) - P'(I,J)\right] \quad (10-a)$$

$$v_{I,j} = v^*_{I,j} + d_{Ij}\left[P'(I,J-1) - P'(I,J)\right] \quad (10-b)$$

Now the discretized continuity equation on the control volume of scalar quantities is written as follows :

$$\left[(\rho uA)_{i+1,J} - (\rho uA)_{i,J}\right] - \left[(\rho vA)_{I,j+1} - (\rho vA)_{I,j}\right] = 0$$

Where an are the size of the corresponding faces.

The introduction of the velocity correction equations (10) in the continuity equation gives a final equation allowing us to determine the scope of pressure corrections P:

$$a'_{IJ} P'(I,J) = a'_{I+1J} P'(I+1,J) + a'_{I-1J} P'(I-1,J) + a'_{IJ+1} P'(I,J+1) + a'_{IJ-1} P'(I,J-1) \quad (11)$$

The algorithm can be summarized as follows : one starts from an initial field P^*, u^*, v^* *and* ϕ^*, with ϕ represents the scalar quantities T, k and Ɛ. Then the system (6) is solved to have new values of u^* *and* v^*.

Then the system (11) is solved for the corrections field pressure P'.

Thereafter, pressure and velocity are corrected by equations (7) and (10) to have P, u and v.

We solve the following transport equation of scalar quantities (2), ϕ = T, K and ε.

Finally, we consider:

$P^* = P ; u^* = u \ ; v^* = v ; \phi^* = \phi .$

And the cycle is repeated until convergence.

IV. RESULTS AND DISCUSSIONS

The dimensions of the channel presented in this work are based on experimental data published by Demartini et al [2]. The air flow is carried out under the following conditions.

- Channel length: L = 0.554 m;
- Channel diameter D = 0.146 m;
- baffle height : 0 <h <0 1. m;
- baffle thickness: δ = 0.01 m ;
- Reynolds number: Re = 8.73 10^4 ;
- The hydrodynamic and thermal boundary conditions are given by :

At the channel inlet:

$u = u_{in}$ =7,8m/s;

$v = 0$; $T = T_{in}$ =300 K

On the channel walls:

$u = v = 0$ and $T = T_w = 373K$

At the channel exit the system is assumed to be fully developed, ie :

$$\partial u / \partial x = \partial v / \partial x = \partial T / \partial x = \quad 0$$

First, we compared the structure of streamlines and isotherms in a channel without baffle with those obtained when we introduce baffle having a height h = 0.05 m (Case 2-1) at the abscise L_1 = 0.218 m. Indeed, in figures 4 and 5 we present streamlines and isotherms for two configurations.

These results clearly show the importance of presence of baffle (acting as a cooling fin). Indeed the baffle increases heat transfer between the wall and the fluid. This increase is caused by recirculation zones downstream of the baffle.

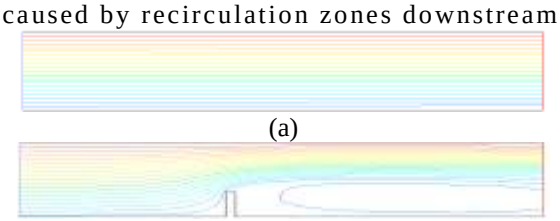

(a)

(b)

Figure 4: **s**treamlines: (a) case 1; (b) case 2-1

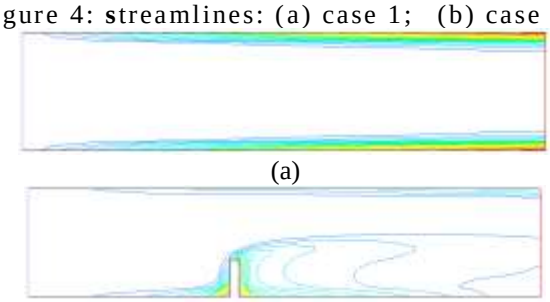

(a)

(b)

Figure 5: Isotherms: (a) case 1; (b) case 2-1

We then studied the influence of baffle height on flow structure and heat transfer. We chose the heights (h = 0.05 m; cases 2-1) h = 0, 073 m (Case 2-2) and h = 0, 1 m (case 2-3).
The figures 6 and 7 present streamlines and isotherms for a channel containing baffle with different heights.

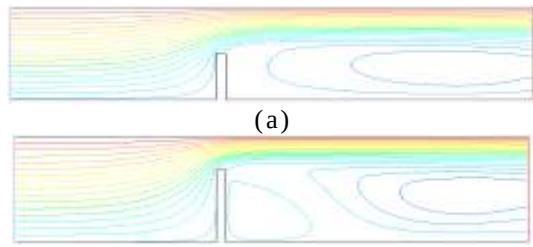

(a)

(b)

Figure 6: streamlines: (a) case 2-2; (b) case 2-3

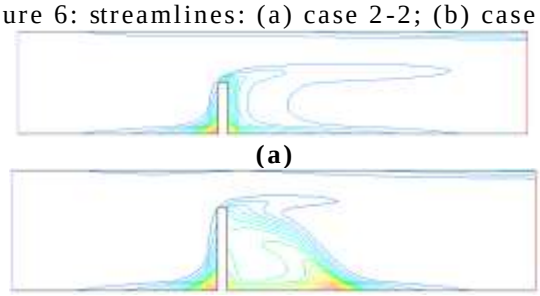

(a)

(b)

Figure 7: Isotherms: (a) case 2-2; (b) case 2-3

It is clear that the isotherms are more condensed near baffle, as and when the height h increases. This indicates an increase of heat transfer near baffle. Indeed, the increase in h expanded exchange area between fluid and walls. In addition, when h increases, the recirculation zone becomes increasingly important (see Figures 4 (b) and figures 6 (a) and (b)). This causes an acceleration of flow, which improves heat transfer within the channel.

We present figures 8 and 9 in order to identify the influence of h on velocities and temperature profiles along y at x = 0.45 from channel inlet. Four values of h are considered.

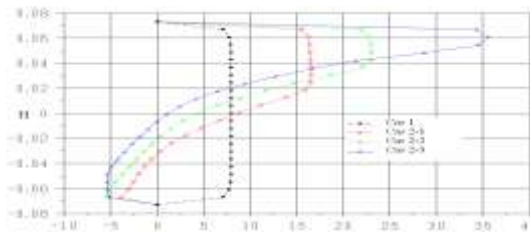

Figure 8: Horizontal velocity Profiles along y at x = 0.45« influence of h »

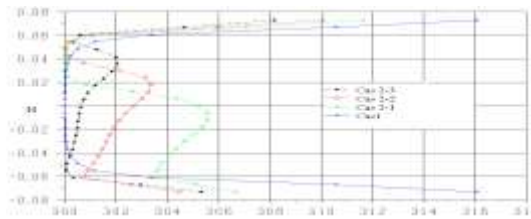

Figure 9: Temperature profiles along y at x = 0.45 m « influence of h »

These results allow us to conclude that the increase of baffle height has two contradictory effects. It is true that there is substantial increase in heat exchange (appearance of recirculation zones most common), but there is also a loss of pressure (flow blockage).

In the purpose of measuring the influence of 'h' on local heat transfer, we have presented in figure 10, the local Nusselt number along the channel for the four cases of h considered. It shows that upstream of the baffle (x <0.2 m) curves are confused , while, just after baffle location, effect of baffle height on Nusselt number become increasingly important away from the baffles.

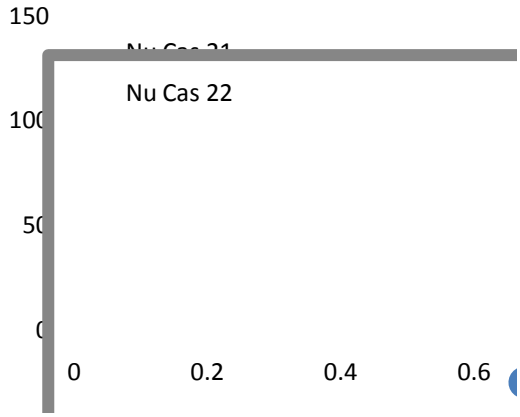

Figure 10 : Local number Nu along the channel « influence of h »

We then studied the influence of baffles number and position 'Figure 11 and 12'.

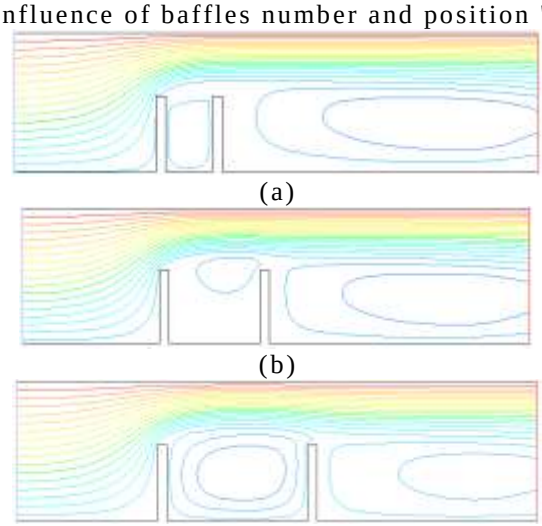

Figure 11 : Streamlines : (a) cas 3-1; (b) cas 3-2; (c) cas 3-3

We consider two baffles of same height h = 0.08 m. The first baffle is placed at the distance $L_1 = 0.15\ m$, while the second is positioned at the distance $d_1 = 0.05$ m from the first (case 3 -1), $d_1 = 0.10$ m (case 3 -2) and $d_1 = 0.15$ m (case 3 -3). We note the existence of two recirculation zones downstream of the first baffle. Also the first recirculation zone 'defined by baffles' becomes increasingly important, which contribute to an increase in heat transfer in this area, as shown in Figure 12. Indeed, when the baffles are close to each other 'd_1 small', the fluid is blocked in the chimney delimited by $x = L_1$ and $x = L_1 + d_1$. This reduces the flow speed at that

location and thus there will be a decrease in the heat transfer in this area. Or when d_1 increases, the fluid has sufficient space to move rapidly, hence heat transfer increases in this zone 'see figure15 '.

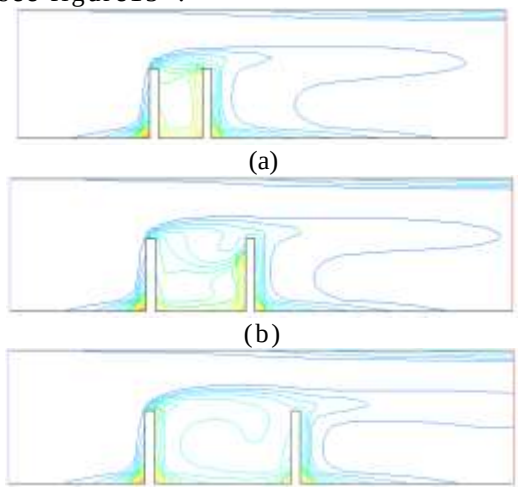

(a)

(b)

(c)

Figure 12 : Isotherms

(a) : « cas 3-1 » ; (b) : « cas 3-2 » ; (c) « cas 3-3 »

In the following figures 13 and 14, we compare the profile of horizontal velocity and temperature distribution. Calculation is done on the y-axis at x = 0.45 m from the channel inlet for three different baffles spacing. We find that more spacing is important more heat exchange is important in areas limited by two baffles.

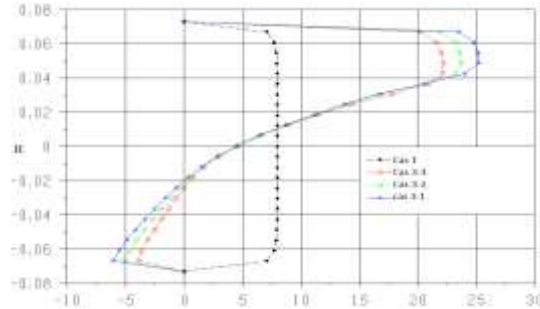

Figure 13 :Profiles of the horizontal velocity at x = 0.45 m « Influence of the spacing between two baffles »

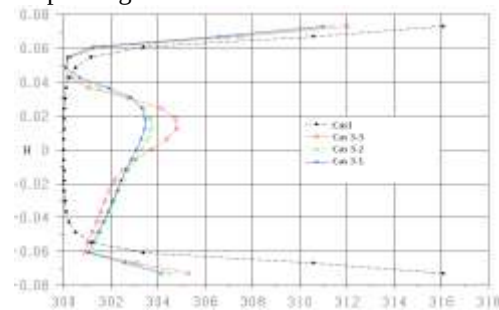

Figure 14: Profiles of the total temperature at x = 0.45 m « Influence of the spacing between two baffles »

Figure 15 present the local Nusselt number along the channel for three considered spacing d_1 = 0.05m, 0.1m and 0.15m.

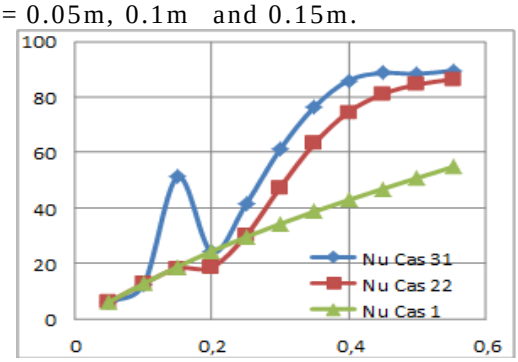

Figure 15 :Local Nusselt number along the channel « Influence of baffles number and position »

We distingue two areas :

The first defined by 0 <x <0.3m while the second by x> 0.3m. For the first region, an increase in number of baffles improves the heat transfer; whereas the reverse is true for the second zone.

We chooses to show the influence of baffles number on heat transfer along the channel for three cases: Channel without baffles, channel containing a single baffle and channel containing two baffles 'Figure 16'.

It should be noted that generally, heat transfer is proportional to baffles number. Indeed, the Nusselt number characterizing heat transfer within the channel increases with increasing baffles number.

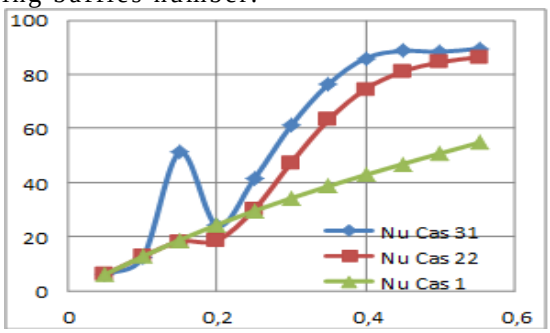

Figure 16: Local Nusselt number along the channel

V. CONCLUSION

The thermal behavior of a stationary turbulent forced convection flow within a baffled channel was analyzed. The results show the ability of our code to predict dynamic and thermal fields in various geometric situations. We studied mainly the influence of baffles height and spacing on heat transfer and fluid flow. One can conclude that:

1 - Increase in the baffle height improves heat transfer between channel walls and fluid passing through it;

2 - Heat transfer becomes increasingly important with adding baffles.

3 - The spacing d_1 between baffles has different effects on local heat transfer. Any time d_1 has not a lot of influence on the overall heat transfer in the channel.

In perspective, we intend deepen and clarify our results. Indeed, we will adapt our code to others geometric cases (non-rectangular baffles or baffles inclined). Finally, we will also try to refine more the turbulence model.

REFERENCES

[1]. S.V.PATANKAR, E.M.SPARROW, « Fully developed flow and heat transfer in ducts having stream wise-periodic variations of cross-sectional area », Journal of Heat Transfer, Vol. 99, p (180-6), 1977.

[2]. L.C.DEMARTNI, H.A.VIELMO and S.V.MOLLER, « Numerical and experimental analysis of the turbulent flow through a channel with baffle plates », J. of the Braz. Soc. of Mech. Sci. & Eng., Vol. XXVI, No. 2, p (153-159), 2004.

[3]. R.SAIM, S.ABBOUDI, B.BENYOUCEF, A.AZZI, « Simulation numérique de la convection forcée turbulente dans les échangeurs de chaleur à faisceau et calandre munis des chicanes transversales », Algérian journal of applied fluid mechanics / vol 2 / 2007 (ISSN 1718 – 5130).

[4]. M. H. NASIRUDDIN, K. SEDDIQUI « Heat transfert augmentation in a heat exchanger tube using a baffle», International journal of Heat and Fluid Flow, 28 (2007), 318-328.

[5]. H.K. Versteeg ; W. Malalasekera « An introduction to computational fluid dynamics » ISBN 0.582-21884-5.

[6]. F. Harlow; J. Welsh ; « Staggered grid », Numerical calculation of time dependent viscous incompressible flow with free surface. Physics of fluids, vol. 8; pp 2182-2189; 1965.

[7]. Patankar, S.V. (1980), «Numerical Heat Transfer and Fluid Flow»,

[8]. Chieng C.C. and Launder B.E. «On the calculation of turbulent heat transport downstream from an abrupt pipe expansion», Numerical Heat Transfer, vol. 3, pp. 189-207.